



Design of weakly-coupled ultra-flattened dispersion few-mode photonic crystal fiber

Xiao Lei¹ · Fang Ren^{1,2}  · Jinyu Zhang¹ · Jingjing Niu¹ · Yanfei Zhang¹ · Yingjuan Ci¹ · Xiaohui Wang¹ · Jianping Wang^{1,2}

Received: 4 November 2021 / Accepted: 18 March 2022 / Published online: 12 April 2022
© The Author(s), under exclusive licence to Springer Science+Business Media, LLC, part of Springer Nature 2022

Abstract

In this paper, a novel design of weakly-coupled few-mode photonic crystal fiber (FM-PCF) supporting 6 vector modes (HE_{11a} , HE_{11b} , TM_{01} , HE_{21a} , HE_{21b} , TE_{01}) with ultra-flattened chromatic dispersion is proposed. We investigate the impact of fiber parameters on chromatic dispersion, minimum effective refractive index difference ($\min\Delta n_{\text{eff}}$), confinement loss, effective mode area, bending loss and nonlinear coefficient. To achieve ultra-flattened chromatic dispersion and large $\min\Delta n_{\text{eff}}$, an extra small elliptical defected hole is introduced in the fiber core. The circular holes in the first ring are replaced by elliptical holes to further obtain flattened-chromatic dispersion. The simulation results show that the chromatic dispersion slope ($< 2.1 \times 10^{-5}$ ns/km/nm²) and large $\min\Delta n_{\text{eff}}$ ($> 6 \times 10^{-4}$) are obtained for the optimized fiber structure. And the proposed FM-PCF has low confinement loss ($< 10^{-4}$ dB/km) and good bending resistance. The proposed fiber can achieve an ultra-flattened chromatic dispersion (< 0.032 ns/nm/km) of 6 vector modes around C-band, and has the potential applications for large-capacity mode division multiplexing communication systems.

Keywords Photonic crystal fiber · Chromatic dispersion · Dispersion slope · Confinement loss · Nonlinearity

1 Introduction

Photonic crystal fiber (PCF) has been a subject of extensive research all over the world owing to the endlessly single mode, high nonlinearity, high birefringence and ultra-flatten dispersion (Hansen et al. 2001; Delgado-Pinar et al. 2007; Matsui et al. 2005; Tsuchida et al. 2007; Birks et al. 1997; Ortigosa-Blanch et al. 2000) PCFs have great design flexibility and can better control optical properties like dispersion, nonlinearity,

✉ Fang Ren
renfang@ustb.edu.cn

¹ School of Computer and Communication Engineering, University of Science and Technology Beijing, Beijing 100083, China

² Beijing Engineering and Technology Research Center for Convergence Networks and Ubiquitous Services, University of Science and Technology Beijing, Beijing 100083, China

birefringence (Ani et al. 2017). Therefore, photonic crystal fiber can realize potential applications, including fiber waveguides, dispersion compensation, lasers, sensors and other fiber devices. Owing to the characteristics of high birefringence, large effective refractive index difference (Δn_{eff}) between adjacent modes and controllable dispersion, photonic crystal fiber has great potential applications in the field of space division multiplexing, especially in the field of weakly-coupled mode division multiplexing.

PCFs with flattened chromatic dispersion have been the target of many researchers in the last few years. In order to achieve this property, the first method is to change the geometric arrangement of air holes in the cladding, including triangular, rectangular and octagonal (Wang et al. 2006; Tan et al. 2009; Razzak et al. 2008; Islam et al. 2012). Another method is to change the refractive index of material by doping the additional materials, such as by doping the germanium (Hoo et al. 2004) and fluorine (Zeleny et al. 2013) in the core of fiber, or by infiltrating low index fluids into selected air holes (Liang et al. 2015; Ebnali-Heidari et al. 2014). And the use of additional materials will undoubtedly increase the difficulties in the manufacturing process. Many designs of PCF to flatten chromatic dispersion have been proposed in recent years. For example, Y. M. Wang et al. (2010) proposed a novel photonic crystal fiber, which had a low confinement loss and small dispersion slope of 10^{-4} dB/km and 2×10^{-6} ns/km/nm². J Sultana. et al. (2018) proposed a novel photonic crystal fiber with five rings of hexagonal structure, which had ultra-high birefringence and near zero flattened dispersion (0.53 ± 0.07 ps/THz/cm). W Gao et al. (2019) proposed a hollow-core photonic crystal fiber with ultra-flattened dispersion. Wang et al. (2021) proposed a new photonic crystal fiber with D-sharped air holes in the core region, which had a flattened dispersion of 0.09 ± 0.28 ps/THz/cm and low confinement loss. However, these photonics crystal fibers only support single fundamental mode, there are few reports on weakly-coupled few-mode photonic crystal fibers.

In recent years, Shi et al. (2017) proposed a novel few-mode photonic crystal fiber with special air holes, which can realize the flattened chromatic dispersion curve by removing part of the air holes in cladding. The designed fiber has many advantages such as being able to support 3 modes and achieving flattened chromatic dispersion curve in the wavelength range of 1530 nm to 1560 nm. But the confinement loss of high order mode is larger than 1 dB/m, and the actual manufacturing will be difficult because of the complexity of fiber structure. Therefore, we propose a weakly-coupled few-mode photonic crystal fiber with ultra-flattened chromatic dispersion, which can support 6 vector modes and the confinement loss $< 10^{-4}$ dB/km. The chromatic dispersion, $\min \Delta n_{\text{eff}}$, effective mode area, bending loss and nonlinear coefficient of the proposed FM-PCF are investigated. Simulation results show that the proposed fiber has a large $\min \Delta n_{\text{eff}}$ ($> 6.0 \times 10^{-4}$) between adjacent modes, and can obtain an ultra-flattened chromatic dispersion (< 0.032 ns/km/nm) and low bending loss ($\sim 10^{-6}$ dB/km). The weakly-coupled few-mode photonic crystal fiber not only can support multiple vector modes and can improve the utilization of vector modes, but also can achieve the flattened dispersion over a broad band owing to the controllable dispersion characteristic. The proposed weakly-coupled few-mode photonic crystal fiber can meet the two advantages of low mode crosstalk and flat dispersion and can improve the communication capacity and communication quality of Mode Division Multiplexing communication systems, which is highly desired for large-capacity Mode Division Multiplexing communication systems.

2 Design of weakly-coupled few-mode hexagonal photonic crystal fiber

The cross section of the proposed weakly-coupled few-mode hexagonal photonic crystal fiber is shown in Fig. 1. The structure is formed by four hexagonal rings of circular air holes and a circular ring of elliptical air holes. An extra small defected elliptical hole (with hole diameter r_a and r_b) is introduced in the fiber core. The pitch and the diameters of the first inner ring and the cladding air holes are Λ , d_{0a} , d_{0b} and d , respectively. The proposed weakly-coupled FM-PCF characteristics are simulated with finite element method (FEM), the background material is silica and its refractive index is calculated by the Sellmeier equation (Xiao et al. 2019),

$$n_{\text{silica}}(\lambda) = \sqrt{\frac{0.6961663\lambda^2}{\lambda^2 - 0.0684043^2} + \frac{0.4079426\lambda^2}{\lambda^2 - 0.1162414^2} + \frac{0.8974794\lambda^2}{\lambda^2 - 9.896161^2} + 1}, \quad (1)$$

where λ is the transmission wavelength. Figure 2 shows the optical field distributions of 6 vector modes of the proposed FM-PCF when $\Lambda = 3.2 \mu\text{m}$, $d/\Lambda = 0.6$, $d_{0a} = 1 \mu\text{m}$, $d_{0b}/d_{0a} = 0.8$, $r_a = 0.8$ and $r_b/r_a = 0.6$. It is observed from Fig. 2 that light is well confined in the core of the proposed FM-PCF.

3 Confinement loss

A part of optical power will leak out of structure in practice, and this loss is called confinement loss which also strongly depends on the structure parameters and its value can be calculated by the formula (Saitoh et al. 2003; White et al. 2001).

$$CL = 8.086 k_0 \text{Im}(n_{\text{eff}}), \quad (2)$$

where $k_0 = 2\pi/\lambda$ is the wavenumber in vacuum, the $\text{Im}(n_{\text{eff}})$ is the imaginary part of effective refractive index, and the unit of CL is dB/km.

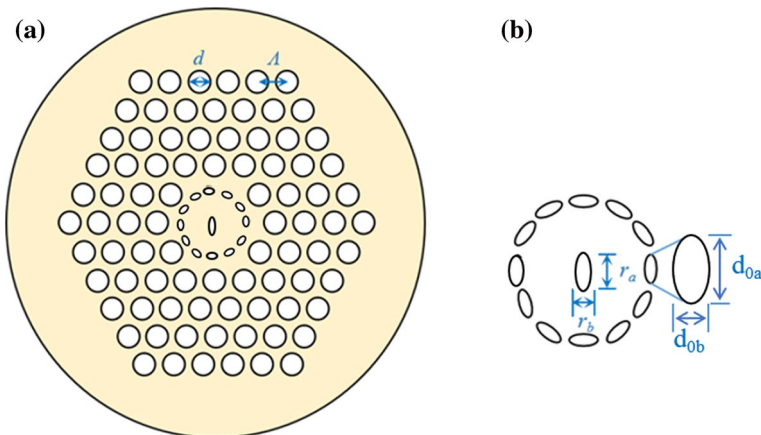


Fig. 1 Cross sectional view **a** and the zoomed core region **b** of the proposed weakly-coupled FM-PCF

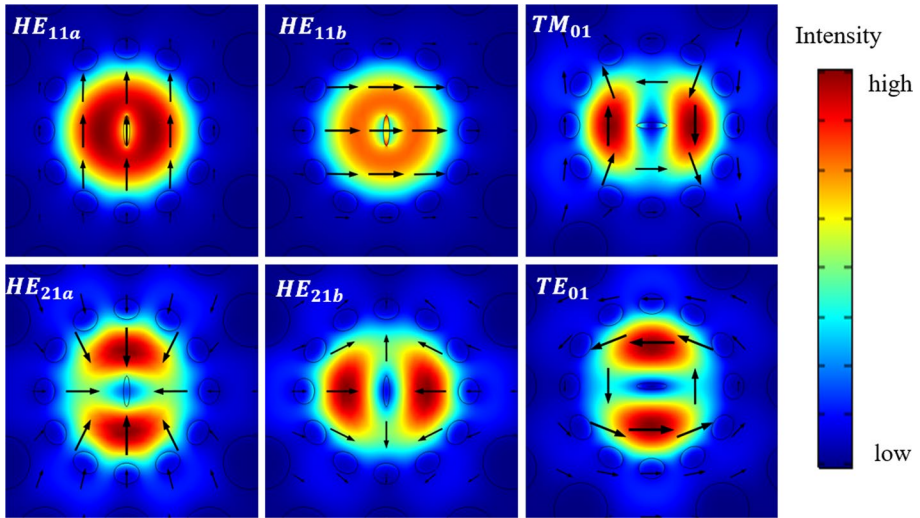


Fig. 2 Optical field distributions of 6 vector modes in the proposed weakly-coupled FM-PCF

4 Chromatic dispersion

The chromatic dispersion is a significant parameter in optical fiber design. And the chromatic dispersion of a PCF fiber can be calculated as the sum of material dispersion D_m and waveguide dispersion D_w (Medjouri et al. 2015),

$$D = D_m + D_w. \tag{3}$$

The material dispersion D_m is derived from the Sellmeier equation (Hansen et al. 2001). The waveguide dispersion is given by the formula,

$$D_w = -\frac{\lambda}{c} \frac{d^2 n_{eff}}{d\lambda^2}, \tag{4}$$

where n_{eff} is the effective refractive index, λ and c represent the wavelength and the speed of light in vacuum, respectively.

5 Effective mode area

A large effective area of mode field can reduce nonlinear effects, the effective mode area A_{eff} is calculated using the definition as (Wang et al. 2015)

$$A_{eff} = \frac{\left[\int_{-\infty}^{+\infty} |E|^2 dx dy \right]^2}{\int_{-\infty}^{+\infty} |E|^4 dx dy}, \tag{5}$$

where E represents the mode field power distribution of the fiber cross section. Meanwhile, the nonlinearity coefficient $\gamma(\lambda)$ of the PCF can be defined as (Saitoh et al. 2005) and the nonlinear coefficient in fibers are inversely proportional to A_{eff} ,

$$\gamma(\lambda) = \frac{2\pi n_2}{\lambda A_{\text{eff}}}, \quad (6)$$

where $n_2 = 3.0 \times 10^{-20} \text{ m}^2 \text{ w}^{-1}$ is the nonlinear refractive index of silica.

6 Differential mode delay

For short-haul transmission systems, the performance of differential mode delay (DMD) is important in terms of reducing the complexing and power consumption. DMD between two adjacent modes can be defined as the value of subtracting the group delay τ_A of τ_B , which is expressed as follows (Ryf et al. 2015):

$$\text{DMD} = \tau_B - \tau_A = n_{gB} - n_{gA} = \frac{n_{\text{eff}B} - n_{\text{eff}A}}{c} - \frac{\lambda}{c} \left(\frac{\partial n_{\text{eff}B}}{\partial \lambda} - \frac{\partial n_{\text{eff}A}}{\partial \lambda} \right), \quad (7)$$

where n_{gA} and n_{gB} are the group indices of mode A and B, c is the light velocity in a vacuum and λ means the free wavelength.

7 Results and discussion

In this part, we adjust the parameters and confirm the influence of one parameter on the properties of the proposed weakly-coupled few-mode PCF to determine a set of comprehensive optimum structure parameters. Firstly, the confinement loss strongly depends on structure parameters, and the confinement loss of each mode in designed weakly-coupled FM-PCF dependent on the number N of air hole rings surrounding the core is shown in Fig. 3. The results show that confinement loss of high order modes is much larger than that of the fundamental mode, and the confinement loss decreases rapidly with N . And the confinement loss of TE_{01} mode is about 29 dB/km for a two-ring PCF, 0.003 dB/km for a three-ring PCF and 1.27×10^{-4} dB/km for a four-ring PCF. The confinement losses of HE_{11a} , HE_{11b} , TM_{01} , HE_{21a} , HE_{21b} and TE_{01} are all below 10^{-4} when N is 5 or bigger. But the confinement loss of HE_{31a} and HE_{31b} are larger than 5 dB/km, which cannot be acceptable for short distance transmission. However, it should be noted that increasing the diameter of cladding by adding more rings of air holes could make the fiber vulnerable, so 5 rings are chosen to find an optimized result. From considerations of manufacturing cost and calculation complexity, we take $N=5$ for the proposed weakly-coupled FM-PCF supporting 6 vector modes.

According to the theory of equivalent refractive index method, the photonic crystal fiber is considered as a fiber with step index profile, and the area occupied by the low refractive index part determines the approximate cladding refractive index. Therefore, as the area of the air hole with low refractive index increases, the relative refractive index difference of the fiber with step index profile similar to the photonic crystal fiber will increase, and the number of propagation modes also increases. Figure 4 indicates the influence of d/Λ and Λ on the minimum effective refractive index difference. The red line and black line

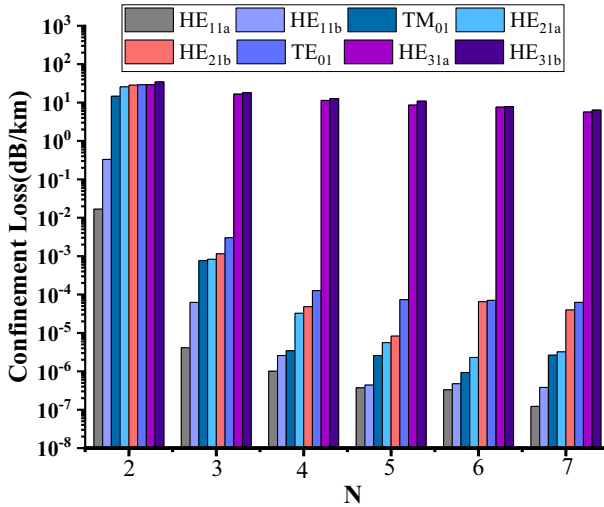
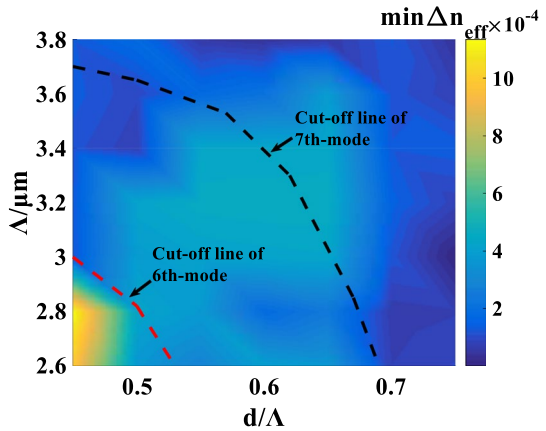


Fig. 3 Confinement losses of the proposed weakly-coupled FM-PCF at $\lambda = 1550$ nm versus the number N of air rings

Fig. 4 Variation of minimum effective refractive index difference $\min\Delta n_{\text{eff}}$ as a function of d/Λ and Λ at $\lambda = 1550$ nm



in Fig. 4 are the cut-off lines of 6th-mode and 7th-mode respectively. Region between the two cut-off lines represents that the proposed weakly-coupled FM-PCF supports 6 vector modes. As shown in Fig. 4, with the increase of the d/Λ , the beam confinement capacity of the defect area increases. Within a certain range, the number of higher-order modes will increase, but if the d/Λ is too large, the $\min\Delta n_{\text{eff}}$ between modes will decrease. Therefore, the air hole diameter cannot be too large, otherwise it will not only increase the coupling between modes, but also effect the fabrication and the structural robustness of fiber. When $d/\Lambda = 0.55 \sim 0.65$ and $\Lambda = 3 \sim 3.4$ μm , the proposed weakly-coupled FM-PCF can support 6 modes and can achieve large $\min\Delta n_{\text{eff}}$ ($> 4 \times 10^{-4}$).

Flat characteristics of chromatic dispersion of the proposed weakly-coupled FM-PCF are affected by the pitch and the diameter of air holes. Firstly, we study the pitch and diameters of air holes to find the optimized ultra-flattened dispersion curve. The chromatic dispersion and dispersion slope curve of the proposed weakly-coupled FM-PCF are shown in

Fig. 5a and b. Figure 5a depicts the chromatic dispersion versus wavelength with different values of the pitch Λ of air holes. As it can be observed, the chromatic dispersion decreases when the Λ decreases, But the flattening of chromatic dispersion also decreases. In order to see the change of dispersion flatness more clearly, the curve of dispersion slope with wavelength is shown in Fig. 5b. It can be seen that when the dispersion is small, the flatness of the dispersion curve is relatively steeper, and when the dispersion is flatter, the dispersion value is slightly larger. To achieve small dispersion and flat dispersion, we choose the point of $\Lambda = 3.2 \mu\text{m}$.

We further extend our study by changing the diameters of air holes to optimize the dispersion and dispersion slope. It is observed from Fig. 6a that the increment of cladding air hole diameters d/Λ up-shifts the dispersion. And Fig. 6b shows that the dispersion slope also increases when the d/Λ increases. With the increases of cladding air hole radius, the dispersion value increases and the dispersion flatness decreases. When $d/\Lambda = 0.6$, the $\min\Delta n_{\text{eff}} = 4.59 \times 10^{-4}$, so the large $\min\Delta n_{\text{eff}}$ of modes and dispersion flatness can be guaranteed near $d/\Lambda = 0.6$.

To focus on the impact of the first ring holes on the dispersion and dispersion slope, we change the diameter of first ring holes d_{0a} , while fixing the other parameters to $\lambda = 1550 \text{ nm}$, $\Lambda = 3.2 \mu\text{m}$, $d/\Lambda = 0.6$, $d_{0b}/d_{0a} = 0.8$, $r_a = 0.8 \mu\text{m}$ and $r_b/r_a = 0.6$. As shown in Fig. 7, with the diameter of the first ring holes d_{0a} increases, the dispersion increases and the dispersion slope decreases. When the diameter of the first ring holes too large, it will cause the loss of fiber modes, so a relatively flattened dispersion can be achieved by choosing $d_{0a} = 1 \sim 1.2 \mu\text{m}$. We further study the influence of ellipticity of the first ring holes on the dispersion and dispersion slope. It can be observed from Fig. 8, only the ellipticity of first ring holes has been changed from 0.6 to 1, while all the other geometric characteristics are kept constant to investigate the impact on chromatic dispersion slope. When the ellipticity $d_{0b}/d_{0a} = 1$, the first ring holes are circular holes and the chromatic dispersion slope is relatively large. And as the ellipticity of the first ring holes increases, the

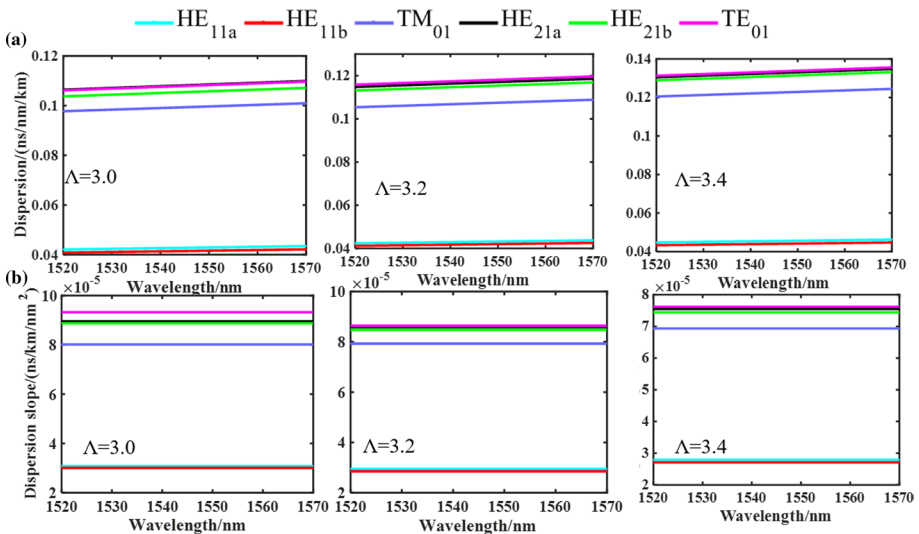


Fig. 5 Variation of chromatic dispersion **a** and chromatic dispersion slope **b** with wavelength for the distance between air holes Λ varying from $3.0 \mu\text{m}$ to $3.4 \mu\text{m}$

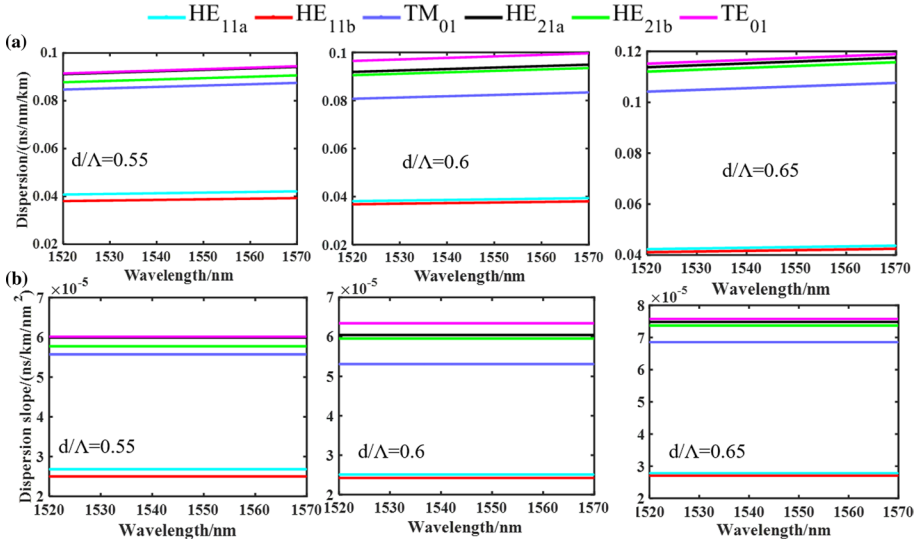


Fig. 6 Variation of chromatic dispersion **a** and chromatic dispersion slope **b** with wavelength for the diameters of cladding air holes d/Λ varying from 0.55 to 0.65

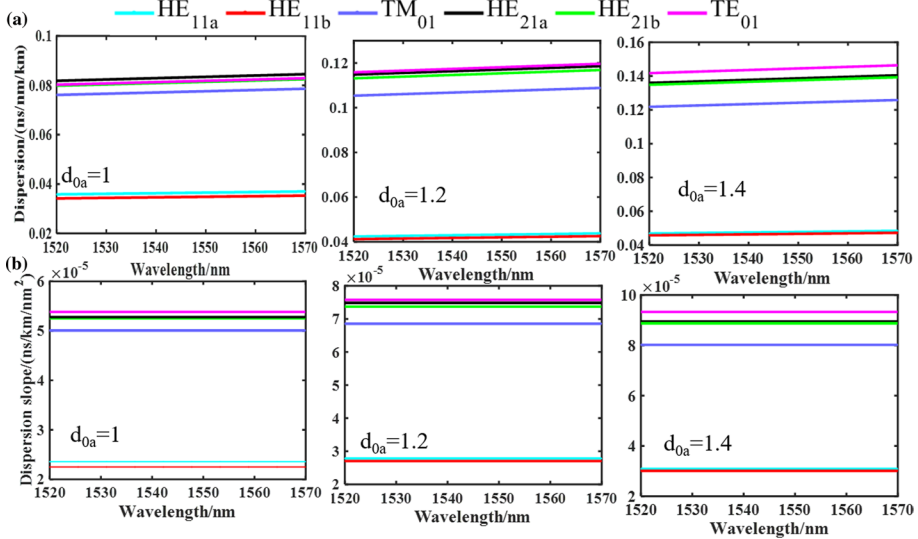


Fig. 7 Variation of chromatic dispersion **a** and chromatic dispersion slope **b** with wavelength for the diameters of the first ring air holes d_{0a} varying from 1 to 1.4 μm

dispersion slope decreases, which indicates that replacing the first circular holes with elliptical holes can further flatten the dispersion. In addition, the influence of diameter of the first ring holes and the ellipticity of air holes on the $\min\Delta n_{\text{eff}}$ is also be investigated. As shown in Fig. 9, the ellipticity of the first ring holes will not increase the effective refractive index difference Δn_{eff} , and when the ellipticity is slightly higher, the $\min\Delta n_{\text{eff}}$ of the

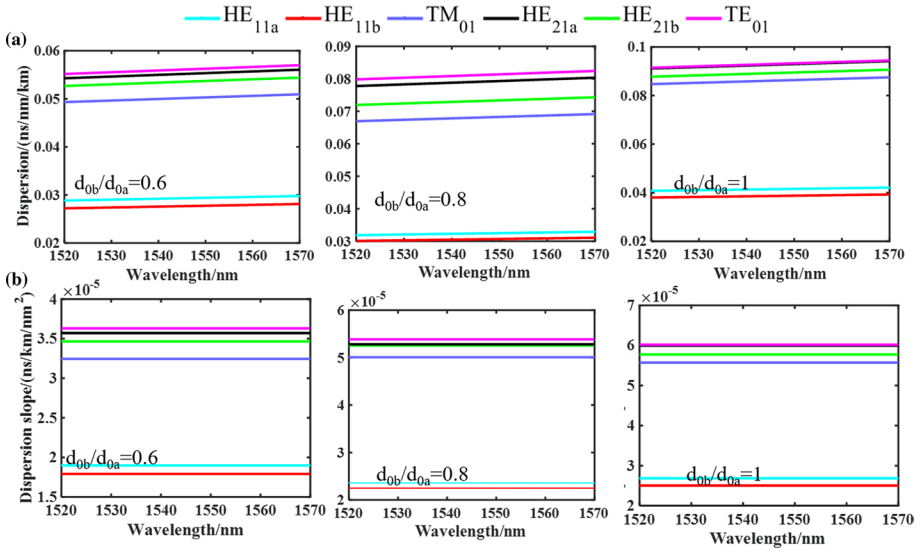
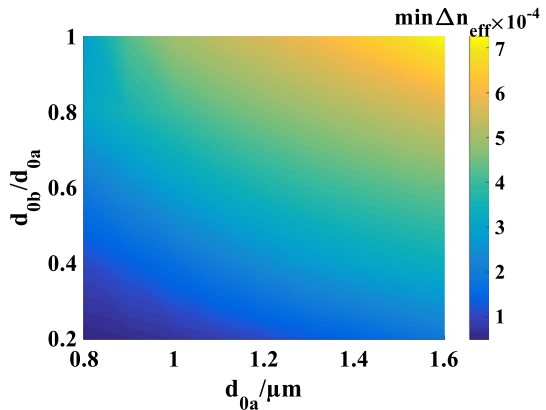


Fig. 8 Variation of chromatic dispersion **a** and chromatic dispersion slope **b** with wavelength for the ellipticity d_{ob}/d_{oa} of the first ring air holes varying from 0.6 to 1

Fig. 9 Variation of minimum effective refractive index difference $\min\Delta n_{eff}$ as a function of diameter d_{oa} and ellipticity d_{ob}/d_{oa} of the first ring holes at $\lambda = 1550$ nm



fiber will be reduced. In order to obtain high minimum effective refractive index difference of modes and flatten dispersion, we chose the point $d_{oa} = 1.2 \mu\text{m}$, $d_{ob}/d_{oa} = 0.8$ as the final design, and the $\min\Delta n_{eff} = 4.8 \times 10^{-4}$, the dispersion < 0.085 ns/nm/km and the dispersion slope $< 5.5 \times 10^{-5}$ ns/km/nm².

Furthermore, we study the influence of the defected air hole in the center of core on the chromatic dispersion and effective refractive index difference. The elliptical design of the defective air hole in the center of core can separate adjacent eigenmodes and increase the Δn_{eff} . As shown in Fig. 10, with the increase of ellipticity r_b/r_a and the diameter of the center defected hole, the $\min\Delta n_{eff}$ increases. And when the $r_a = 0.6 \sim 0.8 \mu\text{m}$, $r_b/r_a = 0.4 \sim 0.8$, the proposed weakly-coupled FM-PCF can achieve large $\min\Delta n_{eff}$ ($> 6 \times 10^{-4}$). The influence of diameter of the central air hole on the dispersion and dispersion slope are shown in Fig. 11a and b respectively. As it can be observed, with the increases of r_a , the dispersion

Fig. 10 Variation of minimum effective refractive index difference $\min\Delta n_{\text{eff}}$ as a function of diameter r_a and ellipticity r_b/r_a of the defected air hole in the center of core at $\lambda = 1550 \text{ nm}$

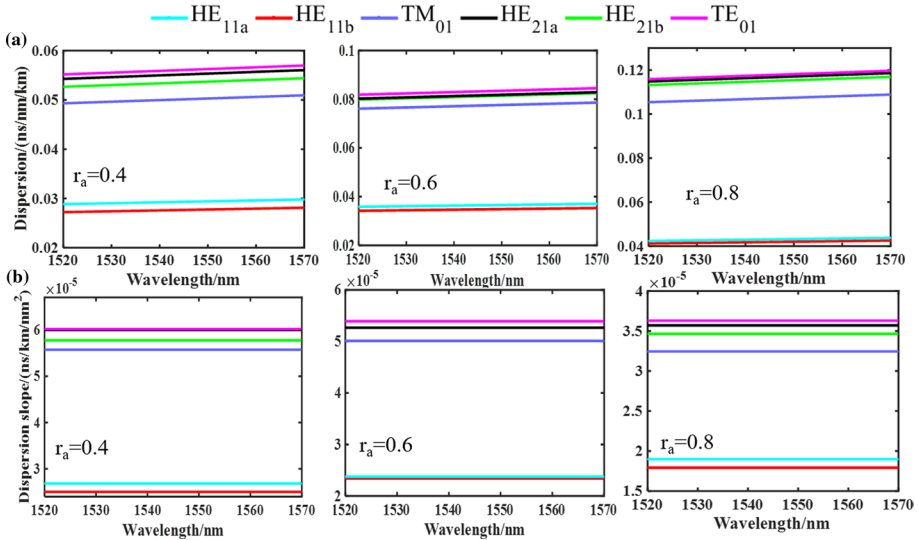
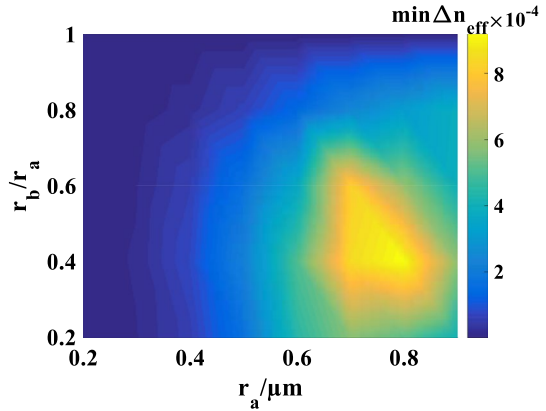


Fig. 11 Variation of chromatic dispersion **a** and chromatic dispersion slope **b** with wavelength for the diameter of the central defected air holes r_a varying from $0.4 \mu\text{m}$ to $0.8 \mu\text{m}$

and the flatness of dispersion increase. In addition, the effect of center defected hole on dispersion flatness is also analyzed. Figures 12a and b show the influence of ellipticity of the defected air hole in the center of core on dispersion and dispersion slope respectively. It is clearly observed that with the value of r_b/r_a from 0.6 to 1, the central air hole gradually becomes round and the dispersion slope curve of the low-order modes moves to point 0. At the same time, compared with the perfectly circular central air hole, the lateral short-axis radius of the elliptical central hole is reduced, so the dispersion value and dispersion slope of some modes is reduced. In order to flatten the dispersion and increase the $\min\Delta n_{\text{eff}}$ of transmission mode, a balance should be found in the elliptical core design. Therefore, a rounder central elliptical air hole is conducive to the flattening of dispersion and increase the $\min\Delta n_{\text{eff}}$ of adjacent vector modes. When $r_a = 0.6 \mu\text{m}$ and $r_b/r_a = 0.8$, the dispersion of HE_{21a} , HE_{21b} and TE_{01} is 0.032 ns/nm/km , 0.031 ns/nm/km and 0.022 ns/

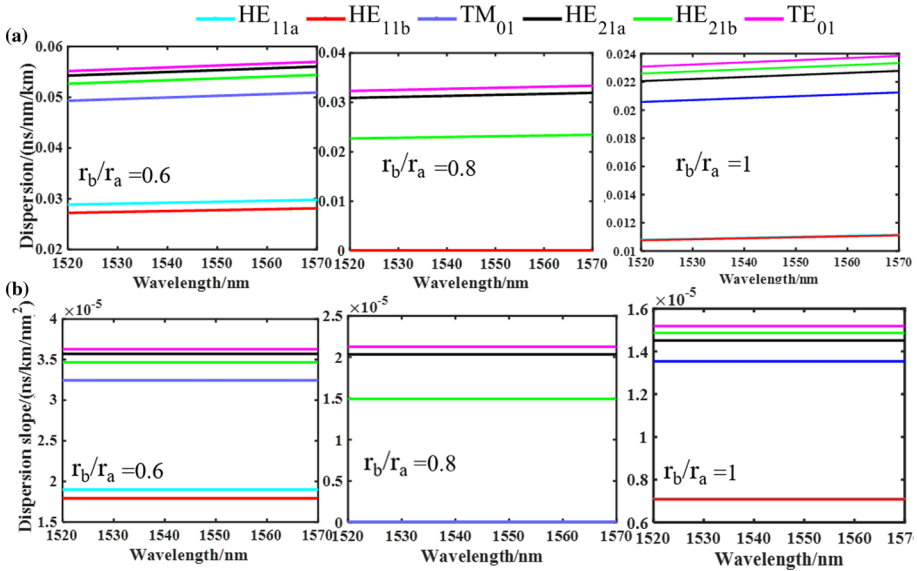


Fig. 12 Variation of chromatic dispersion **a** and chromatic dispersion slope **b** with wavelength for the ellipticity of the central defect air holes r_b/r_a varying from 0.6 to 1

nm/km, respectively. And the dispersion slope of HE_{21a}, HE_{21b} and TE₀₁ is 2.1×10^{-5} , 2.02×10^{-5} and 1.5×10^{-5} , separately. And the dispersion and dispersion slope of HE_{11a}, HE_{11b} and TM₀₁ are 0 over the whole C-band. The simulated results show that the small dispersion and ultra-flattened can be obtained by introducing the defected air hole in the center of core.

From the simulated results on the effects of structure parameters on dispersion and $\min \Delta n_{\text{eff}}$, the optimal structure parameters of the proposed weakly-coupled FM-PCF are set as $\Lambda = 3.2 \mu\text{m}$, $d/\Lambda = 0.6$, $d_{0a} = 1.2 \mu\text{m}$, $d_{0b}/d_{0a} = 0.8$, $r_a = 0.6 \mu\text{m}$, $r_b/r_a = 0.8$. And the corresponding dispersion is lower than 0.032 ns/nm/km and the dispersion slope is lower than 2.1×10^{-5} ns/km/nm² in the range of wavelength from 1520 to 1570 nm.

The effective area A_{eff} and nonlinear coefficients γ of the proposed weakly-coupled FM-PCF within the wavelength range from 1520 to 1570 nm are shown in Fig. 13a and b. From the Fig. 13a, the A_{eff} increases as the wavelength grows, and the A_{eff} of all modes are higher than $15.5 \mu\text{m}^2$ over the whole C-band. Particularly, the A_{eff} of HE_{11a}, HE_{11b}, TM₀₁, HE_{21a}, HE_{21b} and TE₀₁ are $18.5 \mu\text{m}^2$, $18.7 \mu\text{m}^2$, $15.7 \mu\text{m}^2$, $18 \mu\text{m}^2$, $15.8 \mu\text{m}^2$, $18.3 \mu\text{m}^2$ at $\lambda = 1550 \text{ nm}$. As it can be observed from Fig. 13b, with the increases of wavelength, the nonlinear coefficients γ decreases. And the nonlinear coefficients γ of HE_{11a}, HE_{11b}, TM₀₁, HE_{21a}, HE_{21b} and TE₀₁ are $6.5 \text{ w}^{-1} \text{ km}^{-1}$, $6.6 \text{ w}^{-1} \text{ km}^{-1}$, $6.61 \text{ w}^{-1} \text{ km}^{-1}$, $6.8 \text{ w}^{-1} \text{ km}^{-1}$, $7.7 \text{ w}^{-1} \text{ km}^{-1}$ and $7.8 \text{ w}^{-1} \text{ km}^{-1}$ at $\lambda = 1550 \text{ nm}$. And the variation of n_{eff} and the Δn_{eff} with the wavelength are shown in Fig. 14a and b. With the wavelength increases, the n_{eff} of all modes decreases, and the $\min \Delta n_{\text{eff}}$ between all adjacent modes are higher than 6×10^{-4} ($> 10^{-4}$), which indicates that each mode can be independently transmitted.

The variation of bending loss as a function of fiber bending radius is shown in Fig. 15. According to Fig. 15, when the bending radius is small, losses of higher-order modes are more sensitive to the bending radius, and when the bending radius is more than 10 mm, the bending loss of each mode is small than 10^{-6} dB/km. For the few-mode fiber, in addition to

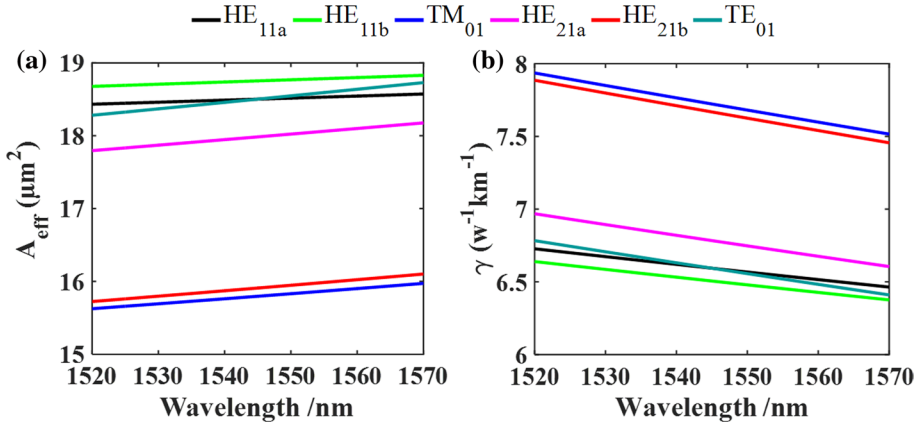


Fig. 13 Variation of effective area **a** and nonlinear coefficients γ **b** with wavelength

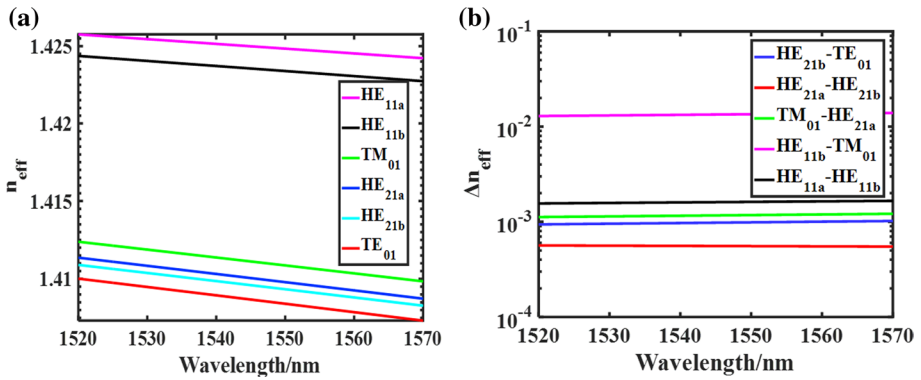


Fig. 14 Variation of n_{eff} **a** and effective refractive index difference Δn_{eff} **b** with wavelength

Fig. 15 Variation of bending loss with the bending radius of the proposed weakly-coupled FM-PCF

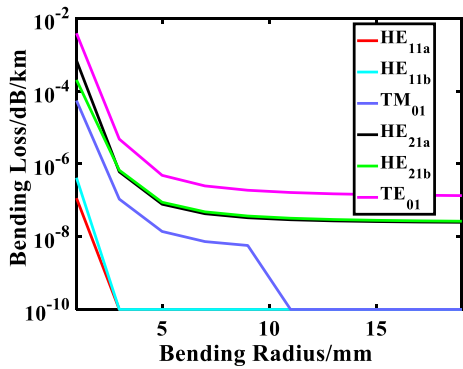
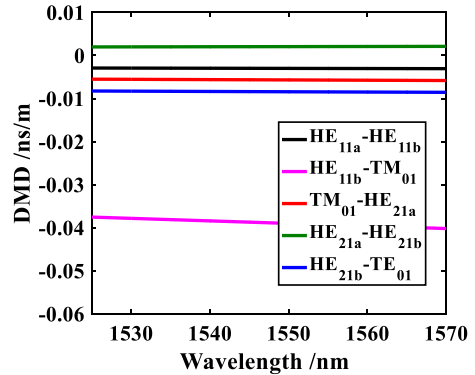


Fig. 16 Variation of differential modal delay DMD with wavelength



the waveguide dispersion and material dispersion generated in transmission, the intermodal dispersion will also limit the transmission capacity of the fiber, so it is also necessary to consider its intermodal dispersion. Figure 16 shows the variation of DMD as a function of wavelength, and the DMD between all adjacent modes exhibit a relatively small DMD (from -0.04 to 0.01 ns/m), which can induce negligible power penalties in short-haul optical communication links. Therefore, the proposed weakly-coupled FM-PCF can be considered to be a promising candidate for MDM systems.

The practical fabrication of the designed FM-PCF based on current fiber manufacture technologies is expected to be achievable. The extrusion technique proposed by Wang J. et al. (2008) offers fabrication freedom for complex structures such as some different complex-shaped asymmetrical air holes. For example, the elliptical-hole structure of the proposed weakly-coupled FM-PCF can be fabricated in polymer material by the extruding and drilling technique (Issa et al. 2004). And the sol-gel casting technique and in-situ polymerization can adjust the pitch and air hole size independently (Zhang et al. 2006; Ma et al. 2015). Therefore, the relatively simple architecture of the proposed weakly-coupled FM-PCF can be fabricated by our extrusion-stretching techniques and we believe that the fabrication of the designed fiber is expected to be realized.

8 Conclusions

In conclusion, a weakly-coupled few-mode ultra-flattened chromatic dispersion photonic crystal fiber supporting 6 vector modes is proposed and its optical properties are investigated by using finite element method. The chromatic dispersion, $\min\Delta n_{\text{eff}}$, confinement loss, effective mode area, bending loss and nonlinear coefficient of the proposed weakly-coupled FM-PCF are investigated. The ultra-flattened chromatic dispersion is achieved by introducing a small defected air hole in the center of core and the first ellipticity holes ring. The numerical results indicate that it can obtain an ultra-flattened dispersion small than 0.032 ns/nm/km with a slight dispersion slope ($< 2.1 \times 10^{-5}$ ns/km/nm²) in the wavelength range of 1520 nm to 1570 nm. Furthermore, the proposed PCF can achieve low confinement loss ($< 10^{-4}$ dB/km), low bending loss ($< 10^{-6}$ dB/km) and large Δn_{eff} ($> 6 \times 10^{-4}$). The proposed fiber can achieve an ultra-flattened chromatic dispersion of 6 vector modes in C-band, and has the potential applications for large-capacity mode division multiplexing (MDM) communication systems.

Funding This work is supported by the Fundamental Research Funds for the Central Universities (FRF-BD-20-11A).

Declarations

Conflict of interest The authors declare no conflicts of interest.

References

- Ani A. B., Faisal M.: Ultra-flattened broadband dispersion compensating photonic crystal fiber with ultra-low confinement loss. International Conference on Electrical & Computer Engineering. IEEE, (2017)
- Birks, T.A., Knight, J.C., Russell, P.S.J.: Endlessly single-mode photonic crystal fiber. *Opt. Lett.* **22**(13), 961–963 (1997)
- Delgado-Pinar, M., Diez, A., Cruz, J.L., Andres, M.V.: High extinction-ratio polarizing endlessly single mode photonic crystal fiber. *IEEE Photon. Technol. Lett.* **19**(8), 562–564 (2007)
- Ebnali-Heidari, M., Saghaei, H., Koohi-Kamali, F., Moghadasi, M.N., Moravvej-Farshi, M.K.: Proposal for supercontinuum generation by optofluidic infiltrated photonic crystal fibers. *IEEE J. Sel. Top. Quant. Electron.* **20**(5), 582–589 (2014)
- Gao, W., Zhang, X., Zhang, Z., Jiang, W., Ohishi, Y.: Numerical investigation on a new designed hollow-core photonic crystal fiber with large modal separation. *Opt. Quant. Electron.* **51**(11), 1–8 (2019)
- Hansen, T.P., Broeng, J., Libori, S.E.B., Knudsen, E., Bjarklev, A., Jensen, J.R., Simonsen, H.: Highly birefringent index-guiding photonic crystal fibers. *IEEE Photon. Technol. Lett.* **13**(6), 588–590 (2001)
- Hoo, Y.L., Jin, W., Ju, J., Ho, H.L., Wang, D.N.: Design of photonic crystal fibers with ultra-low, ultra-flattened chromatic dispersion. *Opt. Commun.* **242**, 327–332 (2004)
- Islam, M.A., Alam, M.S.: Design optimization of equiangular spiral photonic crystal fiber for large negative flat dispersion and high birefringence. *Lightwave Technol.* **30**, 3545–3551 (2012)
- Issa, N.A., Eijkelenborg, M., Fellow, M., Cox, F., Large, M.: Fabrication and study of microstructured optical fibers with elliptical holes. *Opt. Lett.* **29**(12), 1336–1338 (2004)
- Liang, T., Li, W., Feng, G.Y.: Numerical simulation of supercontinuum generation in liquid-filled photonic crystal fibers with a normal flat dispersion profile. *Opt. Commun.* **343**, 196–202 (2015)
- Matsui, T., Zhou, J., Nakajima, K., Sankawa, I.: Dispersion-flattened photonic crystal fiber with large effective area and low confinement loss. *J. Lightwave Technol.* **23**(12), 4178–4183 (2005)
- Ma, T., Andrey, M., Wang, L.L.: Maksim Skorobogatiy, Graded index porous optical fibers dispersion management in terahertz range. *Opt. Expr.* **23**, 7856–7869 (2015)
- Medjouri, A., Simohamed, L., Ziane, O., Boudrioua, A., Becer, Z.: Design of a circular photonic crystal fiber with flattened chromatic dispersion using a defected core and selectively reduced air holes: application to supercontinuum generation at 155 μm . *Photon. Nanostruct. Fundam. Appl.* **16**, 43–50 (2015)
- Ortigosa-Blanch, A., Knight, J.C., Wadsworth, W.J., Arriaga, J., Mangan, B.J., Birks, T.A., Russell, P.S.J.: Highly birefringent photonic crystal fibers. *Opt. Lett.* **25**(18), 1325–1327 (2000)
- Razzak, S.A., Namihira, Y.: Proposal for highly nonlinear dispersion-flattened octagonal photonic crystal fibers. *IEEE Photon. Technol. Lett.* **20**(4), 249–251 (2008)
- Ryf R., Esmaelpour M., Fontaine N.K., et al.: Distributed Raman amplification based transmission over 1050-km few-mode fiber. 2015 European Conference on Optical Communication (ECOC), Valencia, pp. 1–3, (2015)
- Saitoh, K., Koshiba, M.: Leakage loss and group velocity dispersion in air-core photonic bandgap fibers. *Opt. Express* **11**(23), 3100–3109 (2003)
- Saitoh, K., Koshiba, M.: Numerical modeling of photonic crystal fibers. *J. Lightwave Technol.* **23**(11), 3580–3590 (2005)
- Shi W.H., Xu C.X., Jing Y., A new type of few-mode photonic crystal fiber with nearly-zero flattened dispersion properties. 2017 16th International conference on optical communications and networks (ICOCN) (2017)
- Sultana, J., Islam, M.S., Faisal, M., Isiam, M.R.: Highly birefringent elliptical core photonic crystal fiber for terahertz application. *Opt. Commun.* **407**, 92–96 (2018)
- Tan, X.L., Geng, Y.F., Tian, Z., Wang, P., Yao, J.Q.: Study of ultra-flattened dispersion square-lattice photonic crystal fiber with low confinement loss. *Optoelectron. Lett.* **5**(2), 124–127 (2009)
- Tsuchida, Y., Saitoh, K., Koshiba, M.: Design of single-moded holey fibers with large-mode-area and low bending losses. The significance of the ring-core region. *Opt. Express* **15**(4), 1794–1803 (2007)

- Wang, B., Jia, C., Yang, J., Di, Z., Wang, J.: Highly birefringent, low flattened dispersion photonic crystal fiber in the Terahertz region. *IEEE Photon. J.* **99**, 1–1 (2021)
- Wang, J., Jiang, C., Hu, W., Gao, M.: Modified design of photonic crystal fibers with flattened dispersion. *Opt. Laser Technol.* **38**, 169–172 (2006)
- Wang, J., Yang, X.H., Wang, L.L.: Fabrication and experimental observation of monolithic multi-air-core fiber array for image transmission. *Opt Express.* **16**, 7703–7708 (2008)
- Wang Y., Xia Z., Ren X., Long Z. and Huang Y.: Ultra-Flattened Chromatic Dispersion Photonic Crystal Fiber with High Nonlinearity for Supercontinuum Generation. *Communications & Photonics Conference & Exhibition. IEEE*, (2010)
- Wang, X., Lou, S., Lu, W., Sheng, X., Hua, P.: Bend resistant large mode area fiber with multi-trench in the core. *IEEE J. Sel. Top. Quant. Electron.* **22**(2), 1–1 (2015)
- White, T.P., Mcphedran, R.C., Sterke, C.M.D., Botten, L.C., Steel, M.J.: Confinement losses in microstructured optical fibers. *Opt. Lett.* **26**(21), 1660–1662 (2001)
- Xiao, H., Li, H., Wu, B., Dong, Y., Xiao, S., Jian, S.: Elliptical hollow-core optical fibers for polarization-maintaining few-mode guidance. *Opt. Fiber Technol.* **48**(MAR.), 7–11 (2019)
- Zeleny, R., Lucki, M.: Nearly zero dispersion-flattened photonic crystal fiber with fluorine-doped threefold symmetry core. *Opt. Eng.* **52**(4), 602–602 (2013)
- Zhang, Y.N., Li, K., Wang, L.L., Ren, L.Y., Zhao, W., Miao, R.C.: Casting preforms for micro-structured polymer optical fiber fabrication. *Opt. Expr.* **14**, 5541–5547 (2006)

Publisher's Note Springer Nature remains neutral with regard to jurisdictional claims in published maps and institutional affiliations.